

F-μ bond length and μSR depolarization spectrum calculation for fluoride using two-component density functional theory

Zhikang Pan(潘智康), Li Deng(邓力), Ziwen Pan(潘子文), Yue Yuan(原钺), Hongjun Zhang(张宏俊), and Bangjiao Ye(叶邦角)

Citation: Chin. Phys. B, 2023, 32 (**8**): 087602. DOI: 10.1088/1674-1056/acd109
Journal homepage: http://cpb.iphy.ac.cn; http://iopscience.iop.org/cpb

What follows is a list of articles you may be interested in

Atomistic simulations of graphene origami: Dynamics and kinetics

Panpan Zhang(张盼盼), Haihong Jia(贾海洪), Yan-Fang Zhang(张艳芳), and Shixuan Du(杜世萱)
Chin. Phys. B, 2023, 32 (**8**): 087107. DOI: 10.1088/1674-1056/acd527

Site selective 5f electronic correlations in *β*-uranium

Ruizhi Qiu(邱睿智), Liuhua Xie(谢刘桦), and Li Huang(黄理)
Chin. Phys. B, 2023, 32 (**1**): 017101. DOI: 10.1088/1674-1056/ac76ad

Effect of strain on charge density wave order in α-U

Liuhua Xie(谢刘桦), Hongkuan Yuan(袁宏宽), and Ruizhi Qiu(邱睿智)
Chin. Phys. B, 2022, 31 (**6**): 067103. DOI: 10.1088/1674-1056/ac4f4d

Electronic structures, magnetic properties, and martensitic transformation in all-d-metal Heusler-like alloys Cd_2MnTM(*TM*=Fe, Ni, Cu)

Yong Li(李勇), Peng Xu(徐鹏), Xiaoming Zhang(张小明), Guodong Liu(刘国栋), Enke Liu(刘恩克), Lingwei Li(李领伟)
Chin. Phys. B, 2020, 29 (**8**): 087101. DOI: 10.1088/1674-1056/ab9739

Electronic structures of impurities and point defects in semiconductors

Yong Zhang(张勇)
Chin. Phys. B, 2018, 27 (**11**): 117103. DOI: 10.1088/1674-1056/27/11/117103

RAPID COMMUNICATION

F–μ bond length and μSR depolarization spectrum calculation for fluoride using two-component density functional theory

Zhikang Pan(潘智康)[†], Li Deng(邓力)[†], Ziwen Pan(潘子文)[‡],
Yue Yuan(原钺), Hongjun Zhang(张宏俊), and Bangjiao Ye(叶邦角)[§]

State Key Laboratory of Particle Detection and Electronics, University of Science and Technology of China, Hefei 230026, *China*

(Received 29 January 2023; revised manuscript received 25 April 2023; accepted manuscript online 28 April 2023)

First-principles calculation of muons in ionic fluorides has been proposed recently. However, there is a considerable difference between the obtained F–μ bond length and the experimental data obtained by muon spin relaxation (μSR). Considering that the difference may be caused by ignoring the quantum effect of muons, we use two-component density functional theory (TCDFT) to consider the quantized muon and recalculate the bond length and the μSR depolarization spectrum. After testing several muon–electron correlation, we show that TCDFT can give better results than the commonly used "DFT+μ".

Keywords: muon spin relaxation/rotation, fluoride, density-functional theory

PACS: 76.75.+i, 71.15.Mb, 21.60.De **DOI:** 10.1088/1674-1056/acd109

1. Introduction

The μSR technique involves injecting nearly completely polarized muons into the sample and using them as local probe to detect the information of local magnetic field where the muon stops.[1] It is now widely used in physical and chemical investigation of condensed-matter systems.[2] The muon has a positive charge and acts as a proton-like particle in the materials (but only one ninth the mass of proton). After injection into the sample, three processes must be addressed: the muon loses energy until it ends up staying in candidate interstitial sites, local structural relaxation of the atomic positions due to μ^+–sample interaction and the process of spin depolarization of muon under a local magnetic field until decaying (average lifetime $\tau_\mu = 2.2$ μs).[3,4]

Density-functional theory (DFT) has been used to account for the perturbation of the implanted muon to local crystallographic and electronic structures.[5–8] Considering the proton-like muon, a proton can be placed in candidate interstitial sites and the structure is relaxed to estimate the μ^+–sample interaction, while all atoms and the proton are allowed to move until convergence to find the lowest energy site for μ. This method is often referred to as "DFT+μ".[9–13]

In previous work, the depolarization spectrum of muons in ionic fluoride has been simulated based on DFT+μ to study the μ^+–lattice interaction.[14,15] Because of the strong electronegativity of fluoride ions, μ^+ usually stays between two fluoride ions, forming the so-called F–μ–F structure.[16] The DFT+μ results show that there is a significant difference between the calculated F–μ bond length in F–μ–F structure and the expected fitting result of experiment. A common refinement is to consider the quantized muon, phonon method,[3] for example.

In this work, we use the two-component density functional theory (TCDFT), in which both the muon and the electrons are treated as quantized particles thus the quantum effect of the muon can be naturally included by solving the self-consistent field of these two components. We test several different muon–electron two-body correlation energy forms to calculate the convergent muon–electron two-body wave function. Then, the wave function of the muon is used to replace the proton-like muon to calculate the F–μ bond length and the muon depolarization spectrum. The final results show better agreement with the experimental μSR spectrum than DFT+μ, which indicates that the muon wave function and relaxed structure calculated by TCDFT are useful for this kind of research.

2. Structural relaxation of TCDFT method

Recently, TCDFT has been proposed to account for the zero-point motion (ZPM) effect of muons.[17] The wave functions of muon and electrons are separately calculated, the fundamental equations are

$$\left[-\frac{1}{2}\nabla^2 + V_{\text{ion}}^- + V_{\text{H}} + V_{\text{xc}} + V_{\text{coul}}^- + V_{\text{corr}}^-\right]\psi^- = \varepsilon^-\psi^- \quad (1)$$

for the electrons used in DFT and

$$\left[-\frac{1}{2M}\nabla^2 + V_{\text{ion}}^+ + V_{\text{coul}}^+\right]\psi^+ = \varepsilon^+\psi^+ \quad (2)$$

for the muon to obtain the one particle wave function. V_{ion} is the pseudopotential from the ions. V_{H} and V_{xc} are the

[†]These authors contributed equally to this work.
[‡]Corresponding author. E-mail: panzw19@ustc.edu.cn
[§]Corresponding author. E-mail: bjye@ustc.edu.cn

© 2023 Chinese Physical Society and IOP Publishing Ltd

Hartree and exchange–correlation potential for the pseudo-valence charge density. $V_{\rm coul}$ is the Coulomb potential from muon to electrons or from electrons to muon. $V_{\rm corr}$ is the correlation potential from muon to electrons. ψ is the wave function. M is the mass of muon. There is no muon–muon interaction because only one muon is present in the sample at any time.

By varying the Kohn–Sham total energy of the muon–electron–ions system with respect to an atomic position $\boldsymbol{R}_{\rm I}$, the force on atoms can be obtained by[18–20]

$$\boldsymbol{F}_{\rm I} = -\frac{\partial E_{\rm tot}}{\partial \boldsymbol{R}_{\rm I}} = -\sum_{\boldsymbol{k},v} o_{\boldsymbol{k},v} \frac{\delta \varepsilon_{\boldsymbol{k},v}}{\delta \boldsymbol{R}_{\rm I}} + {\rm Tr}\left(\frac{\delta\left(V_{\rm H}+V_{\rm xc}\right)}{\delta \boldsymbol{R}_{\rm I}}\rho\right) - \frac{\partial\left(U+U_{\mu-\rm ions}\right)}{\partial \boldsymbol{R}_{\rm I}}, \tag{3}$$

where $o_{\boldsymbol{k},v}$ is the v-th KS level occupancy at momentum $\boldsymbol{k}$. $\varepsilon_{\boldsymbol{k},v}$ is the KS eigenvalue. U and $U_{\mu-\rm ions}$ are the interatomic and μ–ions Coulomb interaction energies. As the muon is put in the equilibrium position as "DFT+μ"[14,15] suggested and we are not interested in the force on the muon, there is no derivative of the muon position. Using the Hellmann–Feynman theorem, $\delta\varepsilon_{\boldsymbol{k},v}/\delta\boldsymbol{R}_{\rm I}$ of the muon–electron–ions system becomes

$$\frac{\delta \varepsilon_{\boldsymbol{k},v}}{\delta \boldsymbol{R}_{\rm I}} = \left\langle \psi_{\boldsymbol{k},v} \middle| \frac{\delta\left(-\frac{1}{2}\nabla^2 + V^-_{\rm ion} + V_{\rm H} + V_{\rm xc} + V^-_{\rm coul} + V^-_{\rm corr}\right)}{\delta \boldsymbol{R}_{\rm I}} \middle| \psi_{\boldsymbol{k},v} \right\rangle - \varepsilon_{\boldsymbol{k},v} \left\langle \psi_{\boldsymbol{k},v} \middle| \frac{\delta S}{\delta \boldsymbol{R}_{\rm I}} \middle| \psi_{\boldsymbol{k},v} \right\rangle, \tag{4}$$

where S is the projection overlap matrix. Because there is no derivative of muon position, the extra terms over the regular DFT $\left(\partial V^-_{\rm coul}/\partial \boldsymbol{R}_{\rm I}\right.$ and $\left.\partial V^-_{\rm corr}/\partial \boldsymbol{R}_{\rm I}\right)$ are equal to 0.

With only adding the forces of Coulomb interaction of muon–ions

$$\frac{\partial U_{\mu-\rm ions}}{\partial \boldsymbol{R}_{\rm I}} = \frac{\partial\left(\int V_{\rm ions-\mu}(r)\rho_\mu(r)\,{\rm d}r\right)}{\partial \boldsymbol{R}_{\rm I}}, \tag{5}$$

we can obtain the atomic forces to perform structural relaxation. Here $\rho_\mu(r)$ is the density distribution of μ at r, and $V_{\rm ions-\mu}(r)$ is the pseudo potential from the ions to μ.

3. μSR study of ionic fluorides

The F–μ–F structure has attracted new interest in the study of entangled quantum states.[21,21] The spin of μ^+ is strongly coupled with the spin of the magnetic nuclei in the material (especially the two nearest fluorine nuclei), and the polarization of μ^+ then evolves in the material according to the dipole–dipole Hamiltonian

$$\mathcal{H}_{\rm s} = \sum_{i>j} \frac{\mu_0 \gamma_i \gamma_j}{4\pi\hbar \left|\boldsymbol{r}_{ij}\right|^3} \left[\boldsymbol{s}_i \cdot \boldsymbol{s}_j - 3\left(\boldsymbol{s}_i \cdot \hat{\boldsymbol{r}}_{ij}\right)\left(\boldsymbol{s}_j \cdot \hat{\boldsymbol{r}}_{ij}\right)\right], \tag{6}$$

where i and j are the labels of each nuclear spin and the muons, $\boldsymbol{s}_i$ and $\boldsymbol{s}_j$ are spins, $\boldsymbol{r}_{ij}$ is the vector between them, γ_i and γ_j are the gyromagnetic ratios.

The time evolution of the muon's spin for a polycrystalline sample $P^\mu(t)$ can be given by[14]

$$P^\mu(t) = \frac{1}{2}\left\langle {\rm Tr}\left[\boldsymbol{\sigma}^\mu_{\hat{n}} \exp(-{\rm i}\hat{\mathcal{H}}_{\rm s}t/\hbar)\boldsymbol{\sigma}^\mu_{\hat{n}} \exp({\rm i}\hat{\mathcal{H}}_{\rm s}t/\hbar)\right]\right\rangle_{\hat{n}}, \tag{7}$$

where the symbol $\langle\,\rangle_{\hat{n}}$ represents the angular average over $\hat{n}$. $\boldsymbol{\sigma}^\mu_{\hat{n}}$ is the Pauli spin operator for the muon in the direction of $\hat{n}$.

For quantum muon, spin Hamiltonian matrix $\hat{\mathcal{H}}_{\rm s}$ can be numerically made using sampling of its wave function. As the wave function of muon can be well described by Gaussian in axial directions (R-square always above 0.99), we divide the x, y, z axes equally into -3σ, -2σ, …, 3σ respectively and use the μ's density results obtained by TCDFT at that $7\times7\times7$ grids. The corresponding spin Hamiltonian matrix for a quantum muon is obtained by taking the corresponding spin Hamiltonian matrix of the muon on the representative grids, multiplying by the weight of the muon's density and finally adding them.

4. Methods and processes

The electronic part of the calculation is carried out using Quantum Espresso (QE).[23] The calculations were performed in a supercell containing $2\times2\times2$ conventional unit cells and norm-conserving pseudopotentials to model the electronic wave functions of the atoms. As an example, we calculated two fluorides, CaF_2 and α-PbF_2. There are already "DFT+μ" calculations and accurate μSR experiments on these two materials.[14,15] The μ^+ will be put at the "DFT+μ" suggested minimum-energy position.

Although the correlation potential from muon to electrons plays an important role in TCDFT, only two correlation forms have been proposed[17,24] to the best of our knowledge. They are both used for comparison. It is worth noting that the correlation potential from electrons to muons will be considered according to Ref. [24] when using its correlation form. Since the specific correlation functional form has only recently been proposed, we also tried the results without correlation energy for comparison.

The TCDFT loop is shown in Fig. 1. The starting atomic configuration and ψ^-_0 are obtained under proton-like muon approximation (DFT+μ). The starting wave function of the muon is chosen to be Gaussian. Two-body self-consistent loop uses Eqs. (1) and (2). Detailed loop calculation is presented in

Ref. [17]. When two-body iteration convergence is achieved, the atomic forces will be computed, and the lattice structure will relax according to the quick-min Verlet dynamics. The two-body iteration will be repeated under the new lattice structure until ψ^+ reaches convergence. Using the DFT+μ relaxed lattice structure as the starting atomic configuration, the ψ^+ does not change obviously under the convergence threshold of Ref. [17]. This shows that a slight lattice change would not obviously influence the muon's wave function. The TCDFT calculation requires approximately 1080 core-hours on our supercomputer, while the DFT+μ calculation requires approximately 840 core-hours. Considering that our starting atomic configurations are the DFT+μ relaxation results, the total computational consumption of TCDFT is approximately two to three times that of DFT+μ.

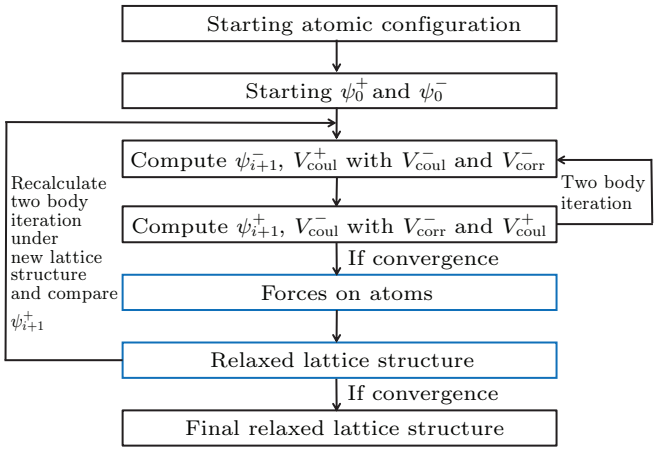


Fig. 1. TCDFT loop. + stands for muon, − stands for electrons. The force calculation is described above.

The self-consistent field total energy convergence threshold is chosen to be 1×10^{-7} a.u. All ions were allowed to relax until the forces on all ions had fallen below a convergence threshold of 2×10^{-3} a.u., and the total energy had fallen below a convergence threshold of 2×10^{-4} a.u.

For CaF_2, the distance from the muon to the two nearest-neighbor fluorines ($r_{\rm nn}$) is needed to fit to the experimental data. A slight change of $r_{\rm nn}$ will cause a significant change in $P(t)$.[16] The concrete lattice structures of CaF_2 and α-PbF_2 with input muons are shown in Fig. 2.

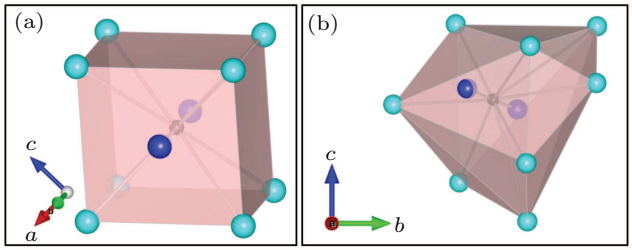


Fig. 2. The input muon in the lowest energy site of (a) CaF_2 and (b) α-PbF_2.[25] The muon (blue sphere) with two nearest-neighbor fluorine nuclei (dark blue spheres) forms F–μ–F structure. And eight weakly coupled next-nearest neighbor fluorine nuclei are represented by cyan spheres.

When not considering the correlation, there is only a slight deviation between the calculated results and the experimental fitting results as shown in Table 1. Using the correlation leads to a greater deviation, and the results using correlation in Ref. [24] are even worse than those using DFT+μ. The reason may be that the harmonic vibration approximation used in Ref. [24] for muonic molecules is not valid for fluorides.[8] As the electron–muon correlation functionals have only been addressed currently, fluoride can provide a precise platform to compare their correctness in ionic crystals.

The α-PbF_2 has a more complicated structure than CaF_2,[25] thus there are four fitting variables for the bond length, and the fitting results are not unique. Reference [15] only selects one best group of fitting results and is shown in Table 2. Compared with the fitting results in Ref. [15], the conclusion is similar to CaF_2, no correlation is the best and the correlation in Ref. [17] can be somewhat better than DFT+μ.

The $A(t)$ is calculated from the $P^{\mu}(t)$ in Eq. (7) using $A(t) = A_0 P^{\mu}(r_{\rm nn}, \zeta; t) + A_{\rm bg}$[14] for CaF_2. Here we are only interested in $r_{\rm nn}$, and the other fitting parameters (A_0 accounts for diamagnetic muons in CaF_2, ζ accounts for magnetic atoms in the infinite lattice and $A_{\rm bg}$ accounts for background

Table 1. Muon-induced structural distortions and variance of the Gaussian distribution of the muon density along the axis in CaF_2. Here the y-axis is chosen as the direction of F–μ–F. The values are obtained by fitting the experimental data,[14] and using DFT +μ and TCDFT.

Parameter	Experiments[14]	DFT+μ[14]	No correlation	Correlation in Ref. [24]	Correlation in Ref. [17]
$r_{\rm nn}$ (Å)	1.172(1)	1.134	1.165	1.122	1.147
σ_x (Å)			0.1162	0.1786	0.1109
σ_y (Å)			0.1058	0.2428	0.1033

Table 2. Muon-induced structural distortions and variance of the Gaussian distribution of the muon density along the axis in α-PbF_2. Here, the cell lengths $a = 6.440$ Å, $b = 3.899$ Å, and $c = 7.651$ Å.[25] The values are obtained by fitting of experimental data,[15] and using DFT+μ and TCDFT.

Parameter	One fit[15]	DFT+μ[15]	No correlation	Correlation in Ref. [24]	Correlation in Ref. [17]
$r_{\rm nn1}$ (Å)	1.1419(4)	1.0967	1.1704	1.0945	1.1105
$r_{\rm nn2}$ (Å)	1.2601(7)	1.2057	1.2204	1.1700	1.2189
$r_{\rm nnn1}$ (Å)	2.68(3)	2.89	2.88	2.89	2.88
$r_{\rm nnn2}$ (Å)	3.01(7)	3.27	3.01	3.01	3.01
σ_x (Å)			0.1137	0.1978	0.1080
σ_y (Å)			0.1207	0.1951	0.1091
σ_z (Å)			0.1173	0.1957	0.1109

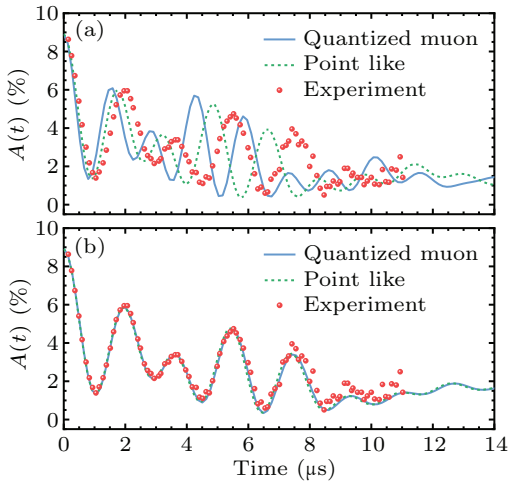


Fig. 3. Muon decay asymmetry data $A(t)$ for polycrystalline CaF_2,[14] simulated with or without the distribution of muons. Here the muon distribution and the corrected bond length are calculated (a) with the correlation of Ref. [24] and (b) without correlation.

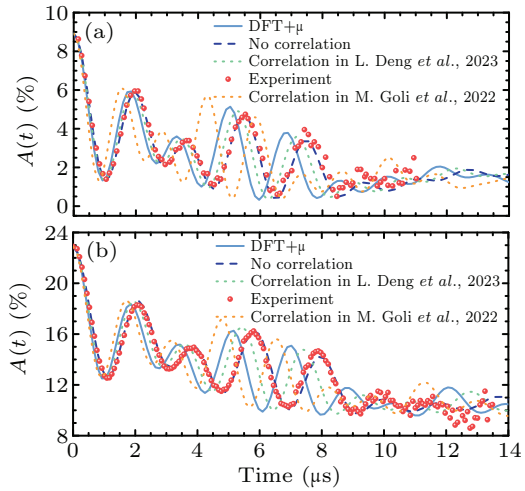


Fig. 4. (a) Muon decay asymmetry data $A(t)$ for polycrystalline CaF_2, together with simulation results. (b) For α-PbF_2. The correlation forms are from Refs. [17,24].

signal) are the same as those in Ref. [14]. For α-PbF_2, fitting parameters other than the F–μ bond length are the same as those in Ref. [15]. The $A(t)$ spectrum of CaF_2 is shown in Fig. 3. No correlation shows good agreements with experiments, and considering the distribution can be slightly improved compered to the point-like case. Note that the muon distribution using the correlation in Ref. [17] is very similar to no correlation case and that a small distribution would not obviously influence $A(t)$. In the case of the correlation in Ref. [24], whether considering the muon distribution would cause a huge difference due to the much wider muon distribution than Ref. [17]. More simulated $A(t)$ with muon distribution is shown in Fig. 4 for both CaF_2 and α-PbF_2. In these two materials, the results become obviously closer to the experiment with the calculated bond length of no correlation. Considering the correlation of Ref. [17] leads to a result far from expected but still better than DFT+μ. This may indicate that the correlation functional is not good enough for the force calculation, but no correlation can be used as a good approximation.

5. Conclusion

In conclusion, we show how quantized muons influence the analysis of the μSR spectrum of fluoride in the framework of TCDFT and try some existing correlation formulas. The calculated spectrum can be much closer to experiments than DFT+μ. However, at present, no correlation shows better agreement than considering the correlation; thus, further study about the correlation is worth. TCDFT shows good potential in the lattice optimization calculation of quantized muons with possible suitable functionals.

Acknowledgement

This work was financially supported by the National Natural Science Foundation of China (Grant No. 12005221).

References

[1] Yang Y X, Chen K W, Ding Z F, Adrian D H and Shu L 2022 *Chin. Phys. Lett.* **39** 107502
[2] Blundell S J 1999 *Contemp. Phys.* **40** 175
[3] Bernardini F, Bonfa P, Massidda S and Renzi D R 2013 *Phys. Rev. B* **87** 115148
[4] Shu L, Ni X J and Pan Z W 2021 *Physics* **50** (in Chinese)
[5] Zhang B, Bao A, Chen C and Zhang J 2012 *Acta Phys. Sin.* **61** 153601 (in Chinese)
[6] Jin R and Chen X H 2012 *Acta Phys. Sin.* **61** 093103 (in Chinese)
[7] Wu H P, Chen D G, Huang D C and Deng K M 2012 *Acta Phys. Sin.* **61** 037101 (in Chinese)
[8] Yang H, Wu M S, Zhang Y, Shi T Y, Varga K and Zhang J Y 2020 *Chin. Phys. B* **29** 043102
[9] Möller J S, Ceresoli D, Lancaster T, Marzari N and Blundell S J 2013 *Phys. Rev. B* **87** 121108(R)
[10] Zhang Y 2018 *Chin. Phys. B* **27** 117103
[11] Guo S L and Ning F L 2018 *Chin. Phys. B* **27** 097502
[12] Yang K W, Li M J, Zhang X J, Li X M, Gao Y L and Long M Q 2017 *Chin. Phys. B* **26** 098509
[13] Liu Y, Liang P, Shu H B, Cao D, Dong Q M and Wang L 2014 *Chin. Phys. B* **23** 067304
[14] Wilkinson J M and Blundell S J 2020 *Phys. Rev. Lett.* **125** 087201
[15] Wilkinson J M, Pratt F L, Lancaster T, Baker P J and Blundell S J 2021 *Phys. Rev. B* **104** L220409
[16] Brewer J H, Kreitzman S R, Noakes D R, Ansaldo E J, Harshman D R and Keitel R 1986 *Phys. Rev. B* **33** 7813(R)
[17] Deng L, Yuan Y, Francis L P, Zhang W S, Pan Z W and Ye B J 2023 *Phys. Rev. B* **107** 094433
[18] Plekhanov E, Bonini N and Weber C 2021 *Phys. Rev. B* **104** 235131
[19] Soler J M, Artacho E, Gale J D, García A, Junquera1 J, Ordejón P and Daniel S P 2002 *J. Phys.: Condens. Matter* **14** 2745
[20] Fan Z Q and Xie F. 2012 *Acta Phys. Sin.* **61** 077303 (in Chinese)
[21] Bonfá P, Frassineti J, Wilkinson J M, Prando G, Isah M M, Wang C N, Spina T, Joseph B, Mitrović V F, Renzi R D, Blundell S J and Sanna S 2022 *Phys. Rev. Lett.* **129** 097205
[22] David B, Edward R, Majdi S, Daniel M, George J W G, Stephen P C, Iain M, Tom L, Michael J G and Sean R G 2022 *Phys. Rev. Lett.* **129** 077201
[23] Giannozzi P, Baroni S, Bonini N, *et al.* 2009 *J. Phys.: Condens. Matter* **21** 395502
[24] Mohammad G and Shant S 2022 *J. Chem. Phys.* **156** 044104
[25] Ehm L, Knorr K, Mädler F, Voigtländer H, Busetto E, Cassetta A, Lausi A and Winkler B 2003 *J. Phys. Chem. Sol.* **64** 919